Statistical mechanics of fluidized granular media: Short-range velocity correlations

R. Soto and M. Mareschal
CECAM, ENS-Lyon, 46 Allée d'Italie, 69007 Lyon, France
(Received 5 July 2000; published 26 March 2001)

A statistical mechanical study of fluidized granular media is presented. Using a special energy injection mechanism, homogeneous fluidized stationary states are obtained. Molecular dynamics simulations and theoretical analysis of the inelastic hard-disk model show that there is a large asymmetry in the two-particle distribution function between pairs that approach and separate. Large velocity correlations appear in the postcollisional states due to the dissipative character of the collision rule. These correlations can be well-characterized by a state dependent pair correlation function at contact. It is also found that velocity correlations are present for pairs that are about to collide. Particles arrive at collisions with a higher probability that their velocities are parallel rather than antiparallel. These dynamical correlations lead to a decrease of the pressure and of the collision frequency as compared to their Enskog values. A phenomenological modified equation of state is presented.

DOI: 10.1103/PhysRevE.63.041303 PACS number(s): 45.70.−n, 05.20.Dd, 05.70.Ln

I. INTRODUCTION

There has been much interest recently devoted to the description of granular media. The understanding of their physical properties is important because they appear in many different phenomena taking place in our daily life as well as in various industrial processes. Experiments have been devised which have permitted one to focus on many different and new aspects. When subjected to injection of energy (vibrated plates, for example), they present many similarities with fluids: convection takes place, patterns can form, and time-periodicity may be observed [1–8].

For those fluidized granular media, careful investigations have permitted one to test the adequacy of hydrodynamical continuum equations generalized to take into account the dissipation of energy due to the inelasticity of the collisions between the grains. Those equations are usually closed with the help of an equation of state and of phenomenological laws inspired by the hard sphere model for fluids [9–14]. Also, kinetic theory models have been studied obtaining good accord with computer simulations in the low density cases [15–17].

In most of these works, granular media are described microscopically by means of the inelastic hard sphere (IHS) model. Grains are modeled as soft hard spheres that dissipate energy at collision through a constant restitution coefficient α. It is quite remarkable that such a simple model can already account for many peculiarities of the observed behavior [18–20].

In this paper we would like to go one step further: namely to investigate the IHS model as if it was a genuine statistical mechanical model for a granular fluid, and examine the effects of the inelasticity on the statistical properties of the fluid. An obvious difference is the absence of any equilibrium state. Left to itself, an assembly of inelastic hard spheres will evolve towards a final state with no motion. One can, however, achieve stationary states by allowing contact with an energy reservoir, but those states are nonequilibrium states with a permanent energy flow coming from the reservoir and dissipated at collisions into the internal elasticity of the grains (and neglected for our purpose). It is our aim to describe these nonequilibrium steady states (NESSs), considering the dissipativity q, defined as $q=(1-\alpha)/2$, as the parameter responsible for deviations from the equilibrium hard sphere system.

Letting a system composed of IHS grains to evolve freely with periodic boundary conditions, it cools down homogeneously. This homogeneous cooling state (HCS) has been widely studied [16,19,21,22], and because of its simplicity the HCS has been used as a reference state to build up theories for nonhomogeneous states. It is the analog of the equilibrium state (with a Maxwellian distribution) for elastic systems [23–25]. Among other features, it has been shown that, in this state, the velocity distribution function is not Maxwellian, having a nonvanishing fourth cumulant and a long velocity tail [22]. Also, long-range velocity correlations are developed in the form of vortex fluctuations [26].

It has been realized that, for any given value of the inelasticity, however small, there is always a size over which the homogeneous reference state loses its stability. The system undergoes a transition towards a state with a shear flow spontaneously developing and possibly towards an inhomogeneous clustered state [11,18,19,27,28]. In order to characterize intrinsic properties like an equation of state, one needs to consider stable homogeneous states before any instability occurs. This means in general to consider slight inelasticities and finite system sizes where $1/N$ effects are present, N being the number of grains.

Computer simulation techniques have proven very valuable in granular studies: as in molecular dynamics (MD), computers are used to integrate numerically the equations of motion of a few hundred to a few thousand grains whose interaction is usually limited to inelastic collisions. The computed behavior compares generally well with experiments, which give confidence in the adequacy of the inelastic hard sphere model to account for most of the specificities of granular fluids. We are going to use such a technique with a mechanism added in order to keep the kinetic energy of the grains constant.

The essential result obtained is the characterization of short-range correlations which are built in granular fluid models and which determine both the static (equation of

state) and dynamical properties (kinetic equation) of the granular fluid. The pressure of the stationary state is computed from its mechanical definition and we can show that it is related to the pair correlation function at contact for precollisional configurations only. This induces an extra variable in the pair correlation function, the angle between relative distance and relative velocity at collision.

Second, the kinetic description of the stationary state is well-described by the (modified) hierarchy equations. In order to write a closed equation for the one-particle distribution function, like the Enskog equation for hard spheres, some assumptions are made on the two particle distribution function. In Enskog's equation, it is assumed that the particles that collide do not have velocity correlations (or dynamical correlations). When two particles are at contact with approaching velocities (precollisional state), it is assumed that the two particle distribution function $f^{(2)}$ can be well-approximated by [29]

$$f^{(2)}(\mathbf{r}_1,\mathbf{v}_1,\mathbf{r}_2,\mathbf{v}_2)\Theta(-\mathbf{v}_{12}\cdot\mathbf{r}_{12})\delta(r_{12}-\sigma) = \chi f^{(1)}(\mathbf{v}_1)f^{(1)}(\mathbf{v}_2)\Theta(-\mathbf{v}_{12}\cdot\mathbf{r}_{12})\delta(r_{12}-\sigma), \quad (1)$$

where $\chi=g(\sigma^+)$ is the pair correlation function at contact and the Heaviside function guarantees that it is a precollisional state. Note that in elastic systems at equilibrium, the previous relation is exact. We show here that this assumption is no longer true for inelastic hard spheres, with an increased probability that colliding disks or spheres are parallel rather than antiparallel, at least for moderately dense fluids. Such velocity correlations might also appear in elastic fluids but only under nonequilibrium regimes (typically over macroscopic scales). Here they appear on the shortest scales, those which correspond to molecular distances, only because of the dissipative character of the microscopic dynamics.

The article is organized as follows: first, we present with some detail the simulation technique which has been used. As already mentioned, we simulate grain dynamics at constant energy: at every collision, all particle velocities are rescaled so as to keep the total kinetic energy constant. We present the technique and emphasize in particular its equivalence with a time-rescaling change. Next we analyze the pressure and the pair-correlation function in the stationary state by making time averages of observables and configurations. The analysis leads in particular to the need to consider velocity correlations which, as will be shown, are also responsible for a pressure drop. This is done in the fourth section, before the conclusions.

II. CONSTANT ENERGY SIMULATIONS OF THE IHS MODEL

In the HCS the system is in a nonstationary state that does not allow one to make time averages of different properties. It is then necessary to inject energy into the system in order to keep it stationary. Different methods have been used, mainly the injection of energy through the walls (vibrating or stochastic), by external fields (like the flow in a pipe), or by stochastic forces acting on the particles (see, for example, [30]). These methods have the disadvantage of destroying the homogeneity of the fluid or, in the case of the stochastic forces, adding other dynamical effects [31].

In this article we use a thermalizing method that both preserves the homogeneity and the dynamical properties of the granular fluid. Formally, each time two particles collide, the dissipated energy is reinjected immediately into the system by multiplying all particle velocities by the same factor. This factor is chosen each time in order to keep kinetic energy constant. As the IHS model does not have an intrinsic energy (or time) scale the rescaling of all velocities does not change the evolution of the system, the collision sequence (thus all physical phenomena) is preserved but viewed at a different speed. In this sense this thermostating mechanism is the most appropriate for the HCS.

In this nonequilibrium steady state (NESS) all macroscopic quantities are stationary and can be averaged in numerical simulations. If we set the initial energy to give a temperature equal to one, then all averaged quantities correspond to computing them at this temperature. To obtain the value at another temperature, simple dimensional analysis gives the desired value. For example, if p_{NESS} is the computed pressure in the NESS, the actual value of the pressure at another temperature T is $p=p_{\mathrm{NESS}}T$.

The IHS model is simulated using event driven molecular dynamics [32]. A direct implementation of the thermalizing method would lead to a computational cost proportional to the total number of particles for each collision, making it impossible to make long simulations. But we can take advantage of the lack of an energy scale to make it much faster. In effect, rescaling all velocities is equivalent to rescaling the time. We define a rescaled time by the relation $ds=\gamma dt$ with

$$\gamma=\sqrt{\frac{E(t)}{E(0)}}, \quad (2)$$

where E is the total energy in the system. Note that γ is a piecewise constant decreasing function. It can be directly checked that if rescaled velocities are defined as $\tilde{\mathbf{v}}=d\mathbf{r}/ds$, then the rescaled kinetic energy ($\tilde{K}=\Sigma m/2\tilde{v}_i^2$) is conserved. This transformation has been successfully used to study the shearing instability [28].

Then, the simulation is done for the cooling IHS model (that is, no velocity rescaling is done) but at each collision the new kinetic energy is computed and γ is evaluated using Eq. (2). In the simulation, then, the energy and the average velocity decrease, but the rescaled velocities are computed using $\tilde{\mathbf{v}}=\mathbf{v}/\gamma$. Having the rescaled velocities, all the static properties can be computed directly. Since the function γ is a piecewise constant function, the s-time can be integrated in the simulation; this allows one to make periodical measurements in the NESS (equally spaced in s).

Finally, to avoid roundoff errors, each time the kinetic energy has decreased by some orders of magnitude (typically 10^{-7} of the initial value) a real velocity rescaling is done to return the temperature equal to one. In this process the center of mass velocity is also subtracted because, otherwise, small errors will be amplified by the rescaling.

As already mentioned the HCS becomes unstable (shearing instability) for certain values of dissipativity, density, and system size. Given values for the dissipativity and density, the system size (number of particles) is constrained to be smaller than a certain value to keep the system homogeneous. In two dimensions for a low density and low dissipation case, it is given by [19]

$$N_{\max}=\frac{\pi}{qn}. \tag{3}$$

For larger densities there are more complex expressions written in terms of the transport coefficients, but in all cases there is a maximum system size over which the system becomes unstable. This phenomenon does not allow one to simulate large systems (for example, for $n=0.2$ and $q=0.02$, $N_{\max}=800$) and finite size effects are obtained. To avoid these effects, simulations with different numbers of particles are done and then the results are extrapolated to the infinite size limit. The extrapolation is done using the standard model for any quantity that does not vanish in this limit, that is, for any quantity A its size dependence is modeled as

$$A(N)=A_\infty+A_1/N. \tag{4}$$

When $N_{\max}$ is smaller than around 1000, the effects of the shearing instability are present before the critical value as fluctuations in the $k=2\pi/L$ mode of the shearing velocity [28]. These fluctuations have both large amplitudes and long correlation times (divergent at the critical point). Some quantities couple strongly with this fluctuating field (for example, the pressure) and small system sizes must be studied to extrapolate to infinity.

We present a series of simulations in two dimensions for the IHS model in the nonequilibrium steady state already described. Dimensions are chosen such that the disk diameter, particle masses, and initial temperature are set equal to one. The simulations are done at three different number densities ($n=N/V$): $n=0.05$, $n=0.1$, and $n=0.2$. In each case the dissipation coefficient takes the values $q=0$, $q=0.002$, $q=0.005$, $q=0.01$, and $q=0.02$. Given the small values of the dissipation coefficients, long simulations are needed to obtain good statistics in order to identify the q-dependence of the different quantities.

As the simulations are done for small dissipations, the results are presented as a series in the coefficient q. Also, when possible, the results are condensed in power expansions in the density, but these expressions must not be interpreted as assuming that these quantities are necessarily analytic in density or dissipativity.

Finally, units are chosen such that the disk diameter σ and the particles masses are set to one. Also, the temperature in the NESS is fixed to one.

III. VIRIAL PRESSURE

As in granular media there is no equivalent to a free energy or an entropy, the pressure cannot be defined thermodynamically but only mechanically. We use the virial expression for the pressure [33] that is a mechanical definition valid for any isotropic system composed of particles that interact with pairwise forces. If the total volume is V and the total kinetic energy is K, in two dimensions the pressure is given by

$$p=\frac{\langle K\rangle}{V}-\frac{1}{4V}\left\langle\sum_{i\neq j}\mathbf{r}_{ij}\cdot\mathbf{F}_{ij}\right\rangle. \tag{5}$$

In the NESS, kinetic energy is constant and equal to N and the forces are impulsive ones. Using the collision rule, it is easy to check that the forces are given by

$$\mathbf{F}_{ij}=-(1-q)|\mathbf{v}_{ij}\cdot\hat{r}_{ij}|\hat{r}_{ij}\delta(t-t_{ij}), \tag{6}$$

where t_{ij} is the collision time for the pair $i-j$, and the relative velocity is evaluated before the collision.

Then, if the average is written as a time average, the delta functions are integrated giving

$$p=n+\frac{1-q}{4V\tau}\sum_{\text{colls}}|\mathbf{v}_{ij}\cdot\mathbf{r}_{ij}|, \tag{7}$$

where τ is the averaging time.

In simulations we measure the quantity

$$p_1=\frac{1-q}{N_{\text{colls}}}\sum_{\text{colls}}|\mathbf{v}_{ij}\cdot\mathbf{r}_{ij}| \tag{8}$$

in terms of which the total pressure is given by

$$p=n+\frac{n\nu}{4}p_1, \tag{9}$$

where ν is the collision frequency.

The results from the simulations fitted linearly with q are

$$\begin{aligned}
p_1(n=0.05)&=1.772(1-q)-0.163q,\\
p_1(n=0.1)&=1.772(1-q)-0.262q,\\
p_1(n=0.2)&=1.772(1-q)-0.528q.
\end{aligned} \tag{10}$$

That collected can be fitted to

$$p_1=\sqrt{\pi}(1-q)-2.67\,qn. \tag{11}$$

The average in Eq. (5) can also be written as an ensemble average

$$\begin{aligned}
p=n+\frac{(1-q)}{4V}\int f^{(2)}(1,2)|\mathbf{v}_{12}\cdot\mathbf{r}_{12}|^2\\
\times\Theta(-\mathbf{v}_{12}\cdot\mathbf{r}_{12})d\mathbf{r}_1d\mathbf{v}_1d\mathbf{v}_2d\theta,
\end{aligned} \tag{12}$$

where θ is the angle between the relative velocity and the relative position. Assuming lack of velocity correlations at collisions, the two particle distribution function can be replaced by Eq. (1). In this case, the integrals can be done explicitly giving

$$p = n + \frac{n^2 \pi (1-q)\chi}{2}. \tag{13}$$

Then, in this approximation, p_1 can be expressed as

$$p_1 = \frac{2n\pi\chi}{\nu}(1-q). \tag{14}$$

To study the validity of this approximation and compare it with the numerical results (11), we need to study the pair correlation function at contact, χ, and the collision frequency, ν.

A. Pair correlation function at contact

For hard particles systems, the pair correlation function at contact χ is defined in elastic systems as $\chi = g(r=\sigma^+)$, where $g(r)$ is the pair correlation function and σ is the particle diameter. In granular media this definition is somewhat ambiguous and a direct application of the classical computational methods [34] to obtain χ does not give the most relevant result.

The pair correlation function is defined in elastic systems as the probability of having two particles separated at a distance r, with an adequate normalization. This definition does not take into account the relative motion of the two particles since it is known that in equilibrium, positions are not correlated with velocities. But, as it is shown below, in granular media, positions and velocities are highly correlated even in the low density limit. The pair correlation function behaves differently if the two particles approach or separate.

In Enskog's kinetic theory, the χ factor that appears in Eq. (1), in the collisional term, in the virial pressure, and in the transport coefficients must be understood as the pair correlation function at contact for particles that are approaching and not for the ones that separate. In what follows we define and describe the basic properties of a generalized χ coefficient that depends on the dynamical state of the particles.

We define the pair correlation function $g(r,\theta)$ as proportional to the number of pairs that are separated by a distance r and there is an angle θ between the relative position and the relative velocity. The normalization is chosen such that g goes to one for large distances. This function is computed in an analogous way as the usual pair correlation function [34]. The generalized pair correlation function at contact $\chi(\theta)$ is defined as $\chi(\theta) = g(r=\sigma^+,\theta)$.

Two classes of pairs can be identified according to the value of the angle θ: if $\cos(\theta)$ is positive then the particles are separating (postcollisional states), and if it is negative the two particles approach (precollisional states). In the Appendix we show that the postcollisional part of $\chi(\theta)$ can be expressed in terms of the precollisional one. Using the collision rule and the conservation of probability during a collision it is found that if $\theta < \pi/2$ (postcollisional)

$$\chi(\theta) = [\cos(\theta)^2 + \alpha^2 \sin(\theta)^2]^{-1} \chi[\pi - \tan^{-1}(\alpha \tan(\theta))], \tag{15}$$

where $[\pi - \tan^{-1}(\alpha \tan(\theta))] > \pi/2$ is the precollisional angle that gives the postcollisional angle θ.

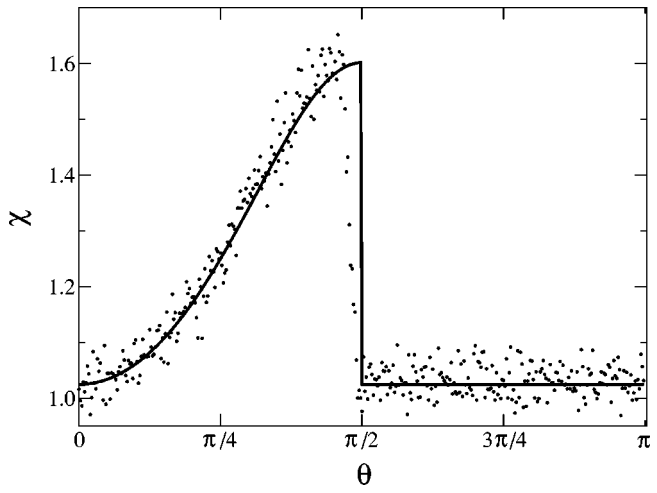

FIG. 1. Estimation of $\chi(\theta)$ obtained in MD simulations (dots) compared to the theoretical prediction. The simulation parameters are $N=1000$, $n=0.02$, and $q=0.1$. The discrepancy near $\theta=\pi/2$ is explained in the text.

In the Enskog approximation, the precollisional pair correlation function is a constant χ_0. In this approximation, the complete function is

$$\chi(\theta) = \begin{cases} \chi_0, & \cos(\theta) \leqslant 0 \\ \chi_0 [\cos(\theta)^2 + \alpha^2 \sin(\theta)^2]^{-1}, & \cos(\theta) > 0. \end{cases} \tag{16}$$

This function is discontinuous at $\theta = \pm \pi/2$. Its average is $\chi_0 \frac{1}{2}(1 + \frac{1}{\alpha})$, which can be understood knowing that the postcollisional normal relative velocity is α times smaller than the precollisional one. That makes that the colliding pair rests $1/\alpha$ times longer in the postcollisional position, giving the previously obtained average (formally the time the particles stay at contact is zero, but χ is the limit of $g(r)$ that can be well-defined for finite bins where the pair stays finite times).

This kind of discontinuity in $\chi(\theta)$ has been found in sheared elastic fluids [29]. In that case the origin of the discontinuity is the nonequilibrium character of the one-particle distribution function. In our case it is originated by the nonconservative collision rule.

The discontinuity in $\chi(\theta)$ makes that the extrapolation of $g(r,\theta)$ to contact presents numerical problems. For the precollisional angles g is a smooth function but for the postcollisional ones there is a discontinuity line arriving at $\theta = \pi/2$ that prevents one from obtaining good estimations of χ for angles slightly below $\pi/2$. In Fig. 1 a numerical estimation of $\chi(\theta)$ obtained in MD simulations for a low density case is presented. The comparison with the Enskog theoretical value [Eq. (16)] is good except for $80° < \theta < 90°$ where it was expected to fail.

In the clustering regime of large systems (where the system is no longer homogeneous) a large dependence of χ on θ has been observed, for the precollisional angles [35,36]. In our case, statistical errors in the results of molecular dynamics simulations do not allow one to determine if there is a

dependence for precollisional angles, contrary to the clear dependence for the postcollisional angles. Nevertheless if χ depends on the precollisional angle, it is small and not like the one reported in the clustering regime.

We define the pair correlation function at contact, χ, as the average of $\chi(\theta)$ over the precollisional angles only. The simulation results for χ, fitted linearly with q, are

$$\chi(n=0.05)=1+0.0655+0.051q,$$

$$\chi(n=0.1)=1+0.1389+0.053q,$$

$$\chi(n=0.2)=1+0.3129+0.070q. \tag{17}$$

An empirical expression for χ in the two-dimensional (2D) elastic case is [37]

$$\chi(q=0)=1+\frac{\pi(25-4n\pi)}{4(4-n\pi)^2}n. \tag{18}$$

A comparison with the measured values show that, for the IHS model, there is a very small dependence on q. Within the statistical error it can be said that χ does not depend on q and its value is the same as in the elastic case.

B. Velocity distribution and collision frequency

It is known that the velocity distribution function for the HCS of the IHS model is not a Maxwellian but a distorted one. In the low velocity region, it is predicted that the fourth cumulant is not zero and using the Boltzmann-Enskog equation its valve has been predicted [22]. The fourth cumulant is defined as

$$k_4=\frac{\langle v^4\rangle-2\langle v^2\rangle^2}{\langle v^2\rangle^2} \tag{19}$$

and the predicted value using the Boltzmann–Enskog equation is for small values of q

$$k_4\approx -2q+22.875q^2. \tag{20}$$

The fourth cumulant is measured in the MD simulations obtaining values consistent with the theoretical predictions.

The collision frequency ν is defined as the average number of collisions per particle and unit s-time. So defined, ν is a stationary quantity. The simulation results fitted linearly with q are

$$\nu(n=0.05)=0.189-0.0042q,$$

$$\nu(n=0.1)=0.403-0.022q,$$

$$\nu(n=0.2)=0.929-0.277q. \tag{21}$$

The collision frequency can be estimated using the approximation that there are no velocity correlations at contact [Eq. (1)]. Taking into account the distortion from the Maxwellian velocity distribution, the collision frequency is given by [22]

$$\nu=2\sqrt{\pi}n\chi\left(1-\frac{k_4}{32}\right), \tag{22}$$

where χ must be understood as the precollisional value.

Both χ and the term $(1-k_4/32)$ have a positive dependence on q, but the MD results (21) show a negative one. This discrepancy shows that the hypothesis of lack of velocity correlations is false and must be modified. Also, when the numerical values for χ [Eq. (17)] and ν [Eq. (21)] are replaced in the approximation (14) for p_1 the predicted pressure is larger than the MD value (11). That is, using the approximation that the two-particle distribution function can be factorized as in Eq. (1) the predicted pressure is larger than the observed one.

IV. VELOCITY CORRELATIONS AT COLLISIONS

Special MD measurements are done to study the source of the discrepancies in pressure and collision frequency. We compute numerically collisional averages sensible to the presence of velocity correlations at contact for precollisional states.

For a system composed of particles that interact with hard core forces, the collision probability is given in two-dimensions by

$$dP_{\mathrm{coll}}(1,2)\propto|\mathbf{v}_{12}\cdot\hat{\boldsymbol{\sigma}}|f^{(2)}(1,2)\,\delta(\mathbf{r}_{12}-\hat{\boldsymbol{\sigma}})\times\Theta(-\mathbf{v}_{12}\cdot\mathbf{r}_{12})d\hat{\boldsymbol{\sigma}}d\mathbf{v}_1d\mathbf{v}_2d\mathbf{r}_1d\mathbf{r}_2, \tag{23}$$

where σ is the particle diameter and Θ is the Heaviside function that restrict the velocities to precollisional states. Collisional averages, defined as the average of any quantity at every collision in the system, can be computed using the previous probability distribution.

$$\langle A\rangle_{\mathrm{coll}(-)}=\frac{1}{n\nu}\int A(1,2)f^{(2)}(12)|\mathbf{v}_{12}\cdot\hat{\boldsymbol{\sigma}}|\times\Theta(-\mathbf{v}_{12}\cdot\hat{\boldsymbol{\sigma}})d\hat{\boldsymbol{\sigma}}d\mathbf{v}_1d\mathbf{v}_2 \tag{24}$$

$$=\frac{1}{n\nu}\int A(1,2)f^{(2)}(12)|\mathbf{v}_2-\mathbf{v}_1|dbd\mathbf{v}_1d\mathbf{v}_2,$$

where b is the impact parameter. The sign $(-)$ in the average means that A is evaluated with the precollisional velocities and that $\mathbf{r}_2=\mathbf{r}_1-\hat{\boldsymbol{\sigma}}$. It must be remarked that the above defined collisional average only takes into account the precollisional part of $f^{(2)}$.

In the hypothesis of absence of precollisional velocity correlations at contact, the two particle distribution function is written as in Eq. (1). As the mean velocity vanishes, this approximation implies that the following collisional average should vanish.

$$\Gamma=\left\langle\frac{\mathbf{v}_1\cdot\mathbf{v}_2}{|\mathbf{v}_2-\mathbf{v}_1|}\right\rangle_{\mathrm{coll}(-)}. \tag{25}$$

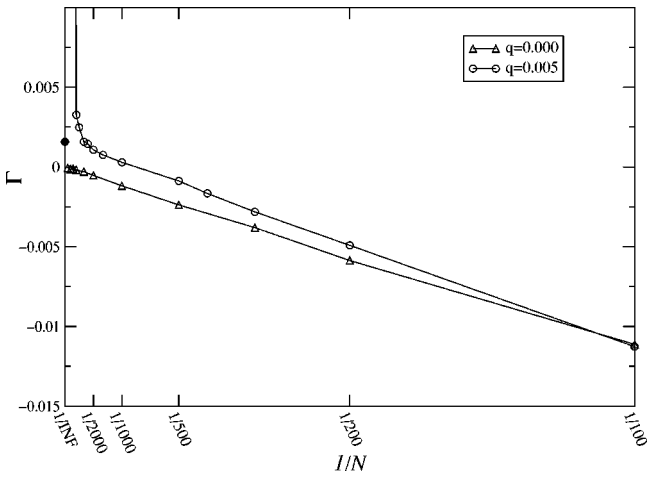

FIG. 2. Values of Γ obtained in MD simulations for an elastic case and a dissipative case as a function of the inverse of the number of particles N. The solid circle indicates the extrapolated value for the dissipative system. The global density is $n=0.1$.

It must be remarked that in an elastic fluid at equilibrium Eq. (1) is exact and Γ must vanish exactly.

This property makes Γ a good test for the hypothesis of the lack of velocity correlations in stationary states. This quantity couples strongly with the velocity fluctuation so careful extrapolation to the infinite system must be done. In Fig. 2 we show the extrapolation procedure for a typical series of simulations. For small system sizes Γ is negative as a consequence of the conservation of total momentum. In finite systems if one particle has a velocity v_0 the others have in average a velocity equal to $-v_0/(N-1)$, leading to negative values for Γ. For large systems, the shearing instability appears giving rise to a dramatic increase of Γ. To get the extrapolated value to infinite system size, we consider systems up to a certain size where no signal of the instability is present ($N=1500$ in the case of the figure).

After extrapolation to infinity system size, the obtained results fitted linearly with q are

$$\Gamma(n=0.05)=0.097q,$$

$$\Gamma(n=0.1)=0.269q,$$

$$\Gamma(n=0.2)=0.442q. \tag{26}$$

That can be collected in the general expression

$$\Gamma=2.29qn. \tag{27}$$

This result means that in effect there are short-range velocity correlations with origins in the dissipative character of the fluid. The fact that the correlation is positive means that particles arrive at collisions with velocities more parallel than if there were no correlations. This phenomenon can be understood in terms of recollisions since, for the IHS model, the velocities of the particles after a collision become more parallel than in the elastic case. This parallelization has two effects: first it increases the probability of having a recollision (that is, after colliding with a third particle the tagged pair recollides) and, second, when the pair recollides, their velocities are correlated, being more parallel. The q dependence and density dependence can be well-understood in this model because the parallelization is proportional to q and the recollision probability to n.

This interpretation is also supported by the results in pressure and collision frequency. In effect, the parallelization of velocities after collisions produces that, in recollisions, the approaching relative velocities are smaller, decreasing the collision frequency. Also the transferred momentum, which averaged gives p_1, is smaller at each collision. The combination of these two effects gives that the velocity correlations produce smaller values for the pressure. The fact that the effects of the correlations in Γ and p_1 are numerically similar is also an indication that the two effects have the same origin.

At low density, precollision velocity correlations are small. This explains the good agreement between the simulations and the theoretical predictions using Enskog's theory for $\chi(\theta)$ in Fig. 1.

Precollisional velocity correlations are also present in elastic fluids, but only under nonequilibrium conditions. Low frequency and long wavelength phenomena (where hydrodynamics is valid) are usually studied as perturbations over local equilibrium states where no velocity correlations exist. In granular fluids, the system is always out of equilibrium and velocity correlations are always present. For a given dissipation, there is no regime with no velocity correlations around which perturbation analysis can be done.

In elastic fluids, the factorization (1) is exact at equilibrium and it allows one to compute static properties like the pressure and the collision frequency. From this starting point, the Enskog equation is built to describe the time evolution of the system in an approximate way (it neglects precollisional velocity correlations in every regime). To mimic the Enskog approach for granular fluids, we should take an equation that includes velocity correlations, even in the HCS, in order to predict accurately the static properties: pressure, collision frequency, and dissipation rate.

At low density and/or dissipation, the velocity correlations are small. Then the Boltzmann–Enskog equation can be used to describe granular fluids with the same degree of approximation as for elastic fluids. For dense dissipative systems more complex theories, that take into account recollisions (for example, ring equations [38,17]), are necessary.

V. CONCLUSIONS

Different properties for the IHS model for granular fluids, put in the homogeneous cooling state, have been carefully studied. Using a time rescaling formalism it was possible to obtain precise averages in MD simulations, allowing one to study the dissipation and density dependence of these properties. Dissipation took values from $q=0$ to $q=0.02$ and number density from $n=0.05$ to $n=0.2$.

In all cases it was found that the velocity distribution is not Maxwellian and the fourth cumulant k_4 is different from zero. Its value does not depend on density and it is in good accord with the kinetic theory predictions.

A distinction is made between the pair correlation function at contact for precollisional and postcollisional states. The first is the one used in kinetic theory (Enskog's theory) and it was found that is has a very small dependence on dissipation, taking the same value than for elastic disks. The postcollisional pair correlation function takes larger values and it can be fully predicted in terms of the precollisional function.

Collisional averages indicate that particles that are about to collide are correlated in a nontrivial way, particles arrive at collisions with velocities that are more parallel than in an elastic fluid. The computed correlation, that is proportional to density and dissipation, has its origin in recollisions: due to dissipation, particles that collide emerge with more parallel velocities than in the elastic case and, when they recollide, their velocities are still more parallel. Results obtained for pressure and collision frequency also show the signature of velocity correlations at collisions. The effect of these correlations is to reduce the collision frequency and the transferred momentum at collisions, thus reducing the virial pressure.

In elastic systems, velocity correlations are also present, but only in nonequilibrium regimes. The intensity of the correlations reduces as the system approaches equilibrium. In granular fluids, on the other hand, the dissipative character of collisions puts the system always out of equilibrium, creating velocity correlations. The observed correlations are intrinsic to granular fluids since they are present in every regine. There is no need for special initial conditions or boundary conditions to obtain and compute them. This allowed us to compute them in a very simple regime, the homogeneous cooling state, with very high precision at the shortest possible scale, the microscopic one.

The presence of these correlations implies that the Enskog factorization (1) is insufficient to compute the static properties of the fluid: pressure, collision frequency, and dissipation rate. For elastic fluids, Enskog's equation, even if it is an approximation, accurately predicts static properties. An equivalent approach for dissipative systems would need the use of a kinetic theory that includes velocity correlations, even in the HCS. More complex theories like ring kinetic theory [38,17] or mode coupling theories [39] are then needed to describe dense granular fluids at finite dissipation.

ACKNOWLEDGMENTS

We wish to thank J. Piasecki for useful discussions. This work was supported by a European Commission DG 12 Grant PSS*1045 and by a grant from FNRS Belgium. One of us (R.S.) acknowledges a grant from MIDEPLAN.

APPENDIX: RELATION BETWEEN THE POST AND PRECOLLISIONAL PART OF $\chi(\theta)$

In this appendix we will deduce the expression (15). The deduction is based on the transformation of the distribution function at collisions and in geometrical aspects of the collision rule.

The instantaneous character of binary collisions in the hard sphere (disk) system implies that the two-particle distribution function can be written as [29]

$$f^{(2)}(1,2)\,\delta(r_{12}-\sigma)=\Theta(-\mathbf{r}_{12}\cdot\mathbf{v}_{12})f_0^{(2)}(1,2) + \frac{1}{\alpha^2}\Theta(\mathbf{r}_{12}\cdot\mathbf{v}_{12})\hat{b}^* f_0^{(2)}(1,2). \tag{A1}$$

The first term is the precollisional distribution function $f_0^{(2)}$. The second term represents the postcollisional distribution function, written in terms of the precollisional one. The operator $\hat{b}^*$ has the effect of replacing the velocities with the precollisional values, and the factor $1/\alpha^2$ comes from the change in relative velocity and the Jacobian of the transformation [17].

The postcollisional part of the pair distribution function is then

$$f^{(2)}(1,2)\Theta(\mathbf{r}_{12}\cdot\mathbf{v}_{12})\,\delta(r_{12}-\sigma) = \alpha^{-2}f_0^{(2)}(1^*,2^*)\Theta(\mathbf{r}_{12}\cdot\mathbf{v}_{12})\,\delta(r_{12}-\sigma), \tag{A2}$$

where 1^* and 2^* represent the state of the particles with precollision velocities.

To simplify notation we will consider a collision in 2D; for the 3D case, the analysis is similar and the results are summarized at the end. The geometry of the collision is represented in Fig. 3. The postcollisional relative velocity is $\mathbf{v}_{12}$, the precollisional relative velocity is $\mathbf{v}_{12}^*$, and σ is the vector that joins the centers of the two particles. The angles θ_1 (precollision) and θ_2 (postcollision) are defined as

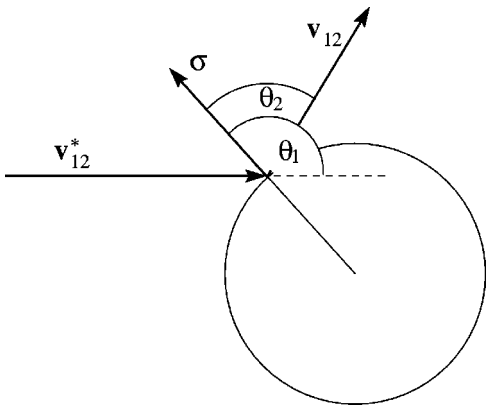

FIG. 3. Geometry of an inelastic collision. $\mathbf{v}_{12}^*$ ($\mathbf{v}_{12}$) is the incoming (outgoing) relative velocity and $\boldsymbol{\sigma}$ is the normal vector to the collision.

$$\theta_1=\cos^{-1}\left(\frac{\mathbf{v}_{12}^*\cdot\sigma}{v_{12}^*}\right), \tag{A3}$$

$$\theta_2=\cos^{-1}\left(\frac{\mathbf{v}_{12}\cdot\sigma}{v_{12}}\right). \tag{A4}$$

The collision rule implies that

$$\tan(\theta_2) = -\alpha^{-1}\tan(\theta_1) \tag{A5}$$

thus

$$\theta_1 = \pi - \tan^{-1}(\alpha \tan(\theta_2)). \tag{A6}$$

The pair correlation function at contact $\chi(\theta)$ is defined as

$$\chi(\theta) = \frac{1}{n^2}\int f^{(2)}(1,2)\,\delta\left[\theta - \cos^{-1}\left(\frac{\mathbf{v}_{12}\cdot\sigma}{v_{12}}\right)\right] d\mathbf{v}_1 d\mathbf{v}_2 d\hat{\boldsymbol{\sigma}}, \tag{A7}$$

where the factor $1/n^2$ guarantees the correct normalization.

For postcollisional angles, $f^{(2)}(1,2)$ can be expressed in terms of the precollisional velocities using Eq. (A2). Changing integration variables we obtain

$$\chi(\theta) = \frac{1}{\alpha n^2}\int f_0^{(2)}(1^*,2^*)\,\delta\left[\theta - \cos^{-1}\left(\frac{\mathbf{v}_{12}\cdot\sigma}{v_{12}}\right)\right] d\mathbf{v}_1^* d\mathbf{v}_2^* d\hat{\boldsymbol{\sigma}}, \qquad \theta < \pi/2, \tag{A8}$$

where it has been used that $d\mathbf{v}_1 d\mathbf{v}_2 = \alpha d\mathbf{v}_1^* d\mathbf{v}_2^*$ [17].

The argument of the delta function can be changed to precollisional velocities using Eqs. (A3), (A4), and (A6)

$$\chi(\theta) = \frac{1}{n^2}[\cos^2(\theta) + \alpha^2\sin^2(\theta)]^{-1}\int f_0^{(2)}(1^*,2^*) \times \delta\left[-\tan^{-1}(\alpha\tan(\theta)) - \cos^{-1}\left(\frac{\mathbf{v}_{12}^*\cdot\sigma}{v_{12}^*}\right)\right] \times d\mathbf{v}_1^* d\mathbf{v}_2^* d\hat{\boldsymbol{\sigma}}, \quad \theta < \pi/2, \tag{A9}$$

where the transformation rule for the delta function has been used. The integral can be identified as the pair correlation function at contact for the precollisional angle $[\pi - \tan^{-1}(\alpha\tan(\theta))]$

$$\chi(\theta) = [\cos^2(\theta) + \alpha^2\sin^2(\theta)]^{-1}\chi[\pi - \tan^{-1}(\alpha\tan(\theta))], \quad \theta < \pi/2 \tag{A10}$$

that is, the postcollisional part of $\chi(\theta)$ can be computed using the precollisional values.

In 3D, we define the pair correlation function that depends on the solid angle $\hat{\Omega}$ that forms the relative velocity and the relative position, where $\hat{\Omega}$ is represented as usual by the angles θ and ϕ. As the tangential components of the relative velocity are preserved at the collision, $\phi_1 = \phi_2$. The change on the normal component of the relative velocity implies the relation (A6). Using the generic relation of the delta function $\delta(\hat{\Omega} - \hat{\Omega}') = \delta(\theta - \theta')\,\delta(\phi - \phi')/|\sin(\theta)|$ and that $|\sin(\theta_1)| = |\sin(\theta_2)|$, it is found by a similar analysis as in the 2D case that

$$\chi(\hat{\Omega}) = [\cos^2(\theta) + \alpha^2\sin^2(\theta)]^{-1}\chi(\hat{\Omega}^*), \quad \theta < \pi/2, \tag{A11}$$

where $\hat{\Omega}^*$ is the precollisional solid angle.

[1] H.J. Herrmann, Physica A **191**, 263 (1992).
[2] K.M. Aoki, T. Akiyama, Y. Maki, and T. Watanabe, Phys. Rev. E **54**, 874 (1996).
[3] F. Melo, P.B. Umbanhowar, and H.L. Swinney, Phys. Rev. Lett. **72**, 172 (1994); **75**, 3838 (1995); P.B. Umbanhowar, F. Melo, and H.L. Swinney, Nature (London) **382**, 793 (1996).
[4] H.M. Jaeger and S.R. Nagel, Science **255**, 1523 (1992); H.M. Jaeger, S.R. Nagel, and R.P. Behringer, Phys. Today **49**, 32 (1996).
[5] E. Falcon *et al.*, Phys. Rev. Lett. **83**, 440 (1999).
[6] L. Kadanoff, Rev. Mod. Phys. **71**, 435 (1999).
[7] R. Wildman, J. Huntley, and J.-P. Hansen, Phys. Rev. E **60**, 7066 (1999).
[8] R. Ramirez, D. Risso, and P. Cordero, Phys. Rev. Lett. **85**, 1230 (2000).
[9] C.S. Campbell, Annu. Rev. Fluid Mech. **22**, 57 (1990).
[10] J.T. Jenkins and S.B. Savage, J. Fluid Mech. **130**, 187 (1983); J.T. Jenkins and M.W. Richman, Arch. Ration. Mech. Anal. **87**, 355 (1985).
[11] P. Deltour and J.-L. Barrat, J. Phys. I **7**, 137 (1997).
[12] K. Helal, T. Biben, and J.P. Hansen, Physica A **240**, 361 (1997).
[13] C. Bizon, M.D. Shattuck, J.B. Swift, and H.L. Swinney, Phys. Rev. E **60**, 4340 (1999).
[14] R. Soto, M. Mareschal, and D. Risso, Phys. Rev. Lett. **83**, 5003 (1999).
[15] C.K.K. Lun *et al.*, J. Fluid Mech. **140**, 223 (1984).
[16] J.J. Brey, F. Moreno, and J.W. Dufty, Phys. Rev. E **54**, 445 (1996).
[17] T.P.C. van Noije and M.H. Ernst, Physica A **251**, 266 (1998).
[18] I. Goldhirsch and G. Zanetti, Phys. Rev. Lett. **70**, 1619 (1993).
[19] S. McNamara and W.R. Young, Phys. Rev. E **53**, 5089 (1996).
[20] E.L. Grossman, T. Zhou, and E. Ben-Naim, Phys. Rev. E **55**, 4200 (1997).
[21] P.K. Haff, J. Fluid Mech. **134**, 401 (1983).
[22] T.P.C. van Noije and M.H. Ernst, Granular Matter **1**, 57 (1998).
[23] R. Ramírez, D. Risso, R. Soto, and P. Cordero, Phys. Rev. E **62**, 2521 (2000).
[24] J.J. Brey, J.W. Dufty, C.S. Kim, and A. Santos, Phys. Rev. E **58**, 4638 (1998).
[25] V. Garzó and J. Dufty, Phys. Rev. E **59**, 5895 (1999).
[26] T.P.C. van Noije, M.H. Ernst, R. Brito, and J.A.G. Orza, Phys. Rev. Lett. **79**, 411 (1997); J.A.G. Orza, R. Brito, T.P.C. van

Noije, and M.H. Ernst, Int. J. Mod. Phys. C **8**, 953 (1997).
[27] J.J. Brey, M.J. Ruiz-Montero, and D. Cubero, Phys. Rev. E **54**, 3664 (1996).
[28] R. Soto, M. Mareschal, and M. Malek Mansour, Phys. Rev. E **62**, 3836 (2000).
[29] J.F. Lutsko, Phys. Rev. Lett. **77**, 2225 (1996).
[30] D.R.M. Williams and F.C. MacKintosh, Phys. Rev. E **54**, R9 (1996).
[31] M. H. Ernst (private communication).
[32] M. Marín, D. Risso, and P. Cordero, J. Comput. Phys. **109**, 306 (1993).
[33] J.-P. Hansen and I. R. McDonald, *Theory of Simple Liquids*, 2nd ed. (Academic, London, 1990).
[34] M. P. Allen and D. J. Tildesley, *Computer Simulation of Liquids* (Oxford Science Publications, Oxford, 1987).
[35] S. Luding, T.A.S.K. Quarterly, Sci. Bull. Acad. Comput. Centre Techn. Univ. Gdansk **2**, 417 (1998).
[36] R. Brito (private communication).
[37] D. Henderson, Mol. Phys. **30**, 971 (1975).
[38] J.R. Dorfman and E.G.D. Cohen, J. Math. Phys. **8**, 282 (1967); M.H. Ernst and J.R. Dorfman, Physica (Amsterdam) **61**, 157 (1972).
[39] Y. Pomeau and P. Resibois, Phys. Rep. **19**, 63 (1975).